Article

Not peer-reviewed version

# Characteristics of radon and thoron indoor and in soil gas and sources of high radon potential in Urumqi, Xinjiang, Northwest China

Nanping Wang *, Jingming Yang , Haochen Wang , Binlin Jia , Aimin Peng

Posted Date: 26 July 2023

doi: 10.20944/preprints202307.1754.v1

Keywords: Indoor radon; soil radon; radon potential; thoron; Urumqi

*Article*

# Characteristics of Radon and Thoron Indoor and in Soil Gas and Sources of High Radon Potential in Urumqi, Xinjiang, Northwest China

**Nanping Wang [1,*], Jingming Yang [2], Haochen Wang [2], Binlin Jia [1] and Aimin Peng [1]**

[1] School of Geophysics and Information Technology, China University of Geosciences (Beijing), 29 Xueyuan Road, Beijing 100083, China; 2010190054@email.cugb.edu.cn (B.J.); paimin@cugb.edu.cn (A.P.)
[2] Geology Party No. 216, China National Nuclear Corporation, 467 Beijing South Road, Urumqi, Xinjiang 830011, China; 21yjm@163.com (J.Y.); hcwong@126.com (H.W.)
* Correspondence: 1996010992@cugb.edu.cn

**Abstract:** Urumqi City, located in the northwest of China, is a city with high indoor radon concentration in nationwide indoor radon survey in China. This study focuses on the assessment of indoor radon level and its potential sources in this city. Indoor radon measure using RAD7 and solid nuclear track detector (SSNTD), soil gas radon by RAD7 and determining specific activity of uranium and radium in soil samples by a high pure germanium spectrometer were performed from 2021 to 2023. The results reveal a wide range of indoor radon concentrations in Urumqi, with anomalies above 400 Bq/m3 in some dwellings. The arithmetical and geometric mean values of indoor radon concentration in Urumqi are 90.24 ± 83.04 Bq/m3 and 66.25 Bq/m3, respectively. The geometric mean values of radon and thoron by SSNTD is 110 Bq/m3 and 109 Bq/m3. The analysis suggest that the activity of faults and fault structures are the main factors influencing indoor radon levels, with frequent earthquakes contributing to higher average radon concentrations. Additionally, investigations into indoor radon and building material radioactivity in detailed are recommended for buildings with radon anomalies and the source of indoor radon anomalies.

**Keywords:** indoor radon; soil radon; radon potential; thoron; Urumqi

## 1. Introduction

Radon ($^{222}Rn$) and thoron ($^{220}Rn$) are radioactive gases generated from the decay of uranium and thorium radioactive series, respectively. Inhaling these radioactive gases and their short-lived decay progenies can damage the respiratory system and increase the incidence of lung cancer. The excess relative risk (ERR) and lung cancer risk due to continuous exposure to high radon concentration in home are comparable to those of miners, indicating a correlation between lung cancer risk and residential radon exposure [1–3]. Global cancer statistics and cancer research reports in China have shown that lung cancer has the highest incidence and mortality rate among malignant tumors [4,5].

Since the late 1970s, extensive research has been conducted worldwide on indoor radon and radon geological potential. It has been found that houses with high radon concentrations are mostly located in areas with high radon geological potential. The indoor radon concentration in a region is related to factors such as near-surface lithology, soil permeability, and geological structures [6–10].

Due to the large land area and budget constraints, China has not yet conducted a detailed national indoor radon assessment project, and research on radon potential mapping in China is generally insufficient. Since the late of 1980s, studies have been conducted on radon and lung cancer, radon potential, and indoor radon levels in areas with high radon geological potential in southern China, such as Yangjiang, Shenzhen, Zhuhai in Guangdong Province, and Gejiu in Yunnan Province [11–15]. In Guangdong, the high indoor radon levels are mainly due to the widespread occurrence of Yanshanian period biotite granite with high uranium, radium, and thorium contents, while in Gejiu, it is mainly caused by the fragmentation of tin ore rocks and tin mining, resulting in high indoor

 doi:10.20944/preprints202307.1754.v1



radon and thoron concentrations [16,17]. In addition, studies have been conducted on radon and thoron concentrations in cave dwellings in Qingyang and Pingliang in Gansu Province [18–20].

Until now four nationwide indoor radon surveys have been conducted in China. From the mid-1980s to 1994, the indoor radon survey was carried out in more than 9,000 dwellings nationwide, and the arithmetic mean of indoor radon concentration was 23.7 Bq/m³ [21,22], mainly using grab sampling with a scintillation chamber. From 2001 to 2004, long-term cumulative measurements of indoor radon were conducted in 20 cities and 6 counties using solid-state nuclear track detector (SSNTD), with a sampling numberof 3,098 homes. The survey results showed that indoor radon concentration in urban areas of China had increased. The arithmetic mean and geometric mean of indoor radon concentration were 43.8 ± 37.7 Bq/m³ and 37.4 Bq/m³, respectively. The number of rooms exceeding 100, 200, and 400 Bq/m³ accounted for 6.4%, 0.7%, and 0.06% of the total surveyed rooms, respectively [23,24]. High indoor radon concentrations were also detected in areas such as Shangrao City in Jiangxi Province and Urumqi City in Xinjiang Autonomous Region [25]. The fourth national indoor radon survey was conducted from 2006 to 2010 using the SSNTD method, covering 2,029 households. The weighted mean concentration was 32.6 ± 5.2 Bq/m³, and the percentage of rooms with radon concentration exceeding 100 Bq/m³ (36 rooms) accounted for 1.8% of the total surveyed rooms [26,27]. The annual average indoor radon concentration in Urumqi was 57 Bq/m³, indicating a relatively high level compared to the national average [26,28,29].

However, in terms of geological background, Urumqi should not be a high radon potential area. in Urumqi, apart from faults and earthquakes, lithology and uranium-radium content in soil should not be the main influencing factors for high indoor radon concentrations.

According to the data from a 1:250,000-scale multi-target regional geochemical survey in the Urumqi-Changji area, uranium and thorium were evenly distributed in surface soil samples in Urumqi, with concentrations of $2.53 \pm 0.13 \times 10^{-6}$ and $9.21 \pm 0.08 \times 10^{-6}$, respectively. The differences in uranium and thorium concentrations among different geological layers are not significant [30]. Moreover, the soil radon concentration in Urumqi was relatively low, with an average value of 3288 Bq/m³ and a range of 45 - 41164 Bq/m³, much lower than the nationwide average of 9614 Bq/m³ in 18 cities [31].

Since both soil uranium content and soil radon concentration are lower than the national average, what makes Urumqi one of the few cities in China with a high indoor radon concentration? Therefore, in order to understand the distribution and characteristics of indoor radon concentration in Urumqi, we conducted indoor radon and soil radon measurements, as well as uranium and radium radioactivity concentration of soil samples, in typical geological structures and densely populated areas of Urumqi from 2020 to 2023, aiming to identify the causes of high radon potential in Urumqi.

## 2. Materials and Methods

### *2.1. Radon and Thoron Measurement*

#### 2.1.1. Instantaneous Radon and Thoron Measurement

In the instantaneous measurement of indoor radon and soil gas, the RAD7 devise with silicon semiconductor made in the United States was adopted. The RAD7 was set with normal mode with 1 h sampling time placed on the table in the living room or the desk in the bedroom at the height of 60 - 80 cm above the ground and a distance more than 30 cm from the wall. In the investigation of radon in soil gas, the RAD7 was set to the sniff mode with a sampling time of 3 min. The soil gas sampling depth was at 80 cm below that ground, and the hole was sealed with soil [32,33].

An Alpha GUARD (PQ2000) served as a reference for comparison measurements and quality control at some indoor radon measuring sites. The instrument was set to flow mode with 10 min. sampling time.

All of the instruments were calibrated annually in the Radon Chamber National Institute of Metrology, China.

 doi:10.20944/preprints202307.1754.v1



#### 2.1.2. Long-term Radon and Thoron Measurement

The long-term measurements using passive integrated radon–thoron discriminative detectors were carried out by an LD-P detectors, a kind of solid-state nuclear track detector (SSNTD). The detector consisted of two diffusion cups for both $^{222}Rn$ and $^{220}Rn$, with built-in two CR-39 films produced by Japan's FUKUVI Chemical Company [34]. Prior to use, the detector was calibrated at the University of South China.

During the investigation, the LD-P detectors, fixed to the edge of a writing desk or a closet in the bedroom at the distances of 5 cm from the wall and 80 - 90 cm above the ground, were deployed for 90 days from January to April in winter.

### *2.2. Soil Sample Collection*

Soil samples were collected at the location where soil radon measurements were made. After removing surface weeds and rocks, soil samples were collected using a ring knife, a cylindrical aluminum box (φ5.5×5cm). A minimum of 1000 g of soil was collected. The soil samples were then sealed in plastic sealing bags, and information such as the sampling site number, soil types, and vegetation on the surface were recorded.

### *2.3. Determination of Specific Activity of Radionuclides in Soil*

The specific activity of radionuclides, including uranium, radium, thorium, and cesium, present in soil samples was determined using the HPGe digital wide-energy gamma-ray spectrum measurement system made by CANBERRA. The detector model is BE3830, and its energy resolution for $^{60}Co$ is 1.68 keV (for 1332.5 keV energy peak). The extended uncertainties for uranium (63.3 and 92.4 keV), radium (351.9 and 609.3 keV), thorium (583.2 and 911.2 keV), and cesium (661.7 keV) were 5.6%, 5.0%, 5.4% and 4.1%, respectively. calibrated using a volume reference source (φ75×70mm) provided by National Institute of Metrology, China.

After transported to the laboratory, the sample was pretreated and analyzed following the guidance of 'Gamma-ray spectrometry method for the determination of radionuclides in environmental and biological samples' [35].

### *2.4. Geological Overview of the Study Area and Sampling Site Selection*

#### 2.4.1. Geographic and Climatic Features

Urumqi City is located between 86°37'33" - 88°58'24" east longitude and 42°45'32" - 45°00'00" north latitude in the northwest of China. Urumqi is situated at the northern foot of the Tianshan Mountains, on the southern edge of the Junggar Basin, surrounded by mountains on three sides, with more than 50% of its total area being mountainous terrain. The northern part consists of a small alluvial plain, which accounts for less than one-tenth of the total area. The city has a permanent population of 4.0824 million people [36]

Urumqi City has a temperate continental climate with semi-arid characteristics. The hottest months are July and August, with an average temperature of 25.7 ℃. The coldest month is January, with an average temperature of -15.2 ℃. The summer is hot and dry, while the winter is cold and long [37].

#### 2.4.2. Geological Overview

The main exposed strata in Urumqi are Upper Carboniferous, Permian, Triassic, Jurassic, Cretaceous, Tertiary and Quaternary, and their lithology mainly includes sandstone, siltstone, conglomerate and mudstone, while the Quaternary sediments are mainly alluvial gravel, silty sand and sandy soil.

Due to its location at the junction of the Bogda Arcuate Uplift Belt and the Urumqi Mountain Front Depression at the southern edge of the Junggar Basin, Urumqi City is characterized by the convergence of multiple tectonic belts, resulting in complex geological structures and intense tectonic

Preprints (www.preprints.org) | NOT PEER-REVIEWED | Posted: 26 July 2023 doi:10.20944/preprints202307.1754.v1



activity. The region is prone to frequent moderate to strong earthquakes. Major fault systems in the area include near-east-west trending faults (the Fukang South Fault and the Xishan Fault), north-east faults (theYamalike-Shuimogou Fault, the Wanyao Gou Fault, and the Bagang-Shihua Concealed Fault), as well as near-north-south trending concealed faults related to the Urumqi River [38–41]. A simplified geological map of Urumqi City (1:10000) with location of radon measurements is shown in Figure 1.

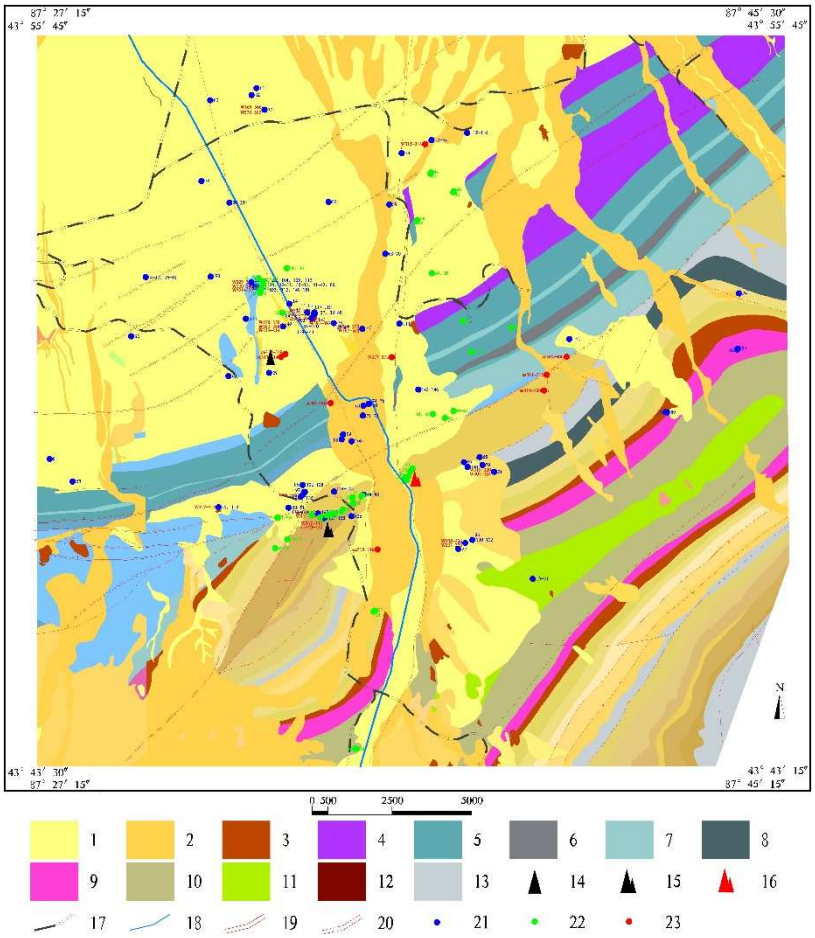


**Figure 1.** A simplified geological map of Urumqi City (1:10000) with location of radon measurements: 1—$Q^h$: sandy fine-medium gravel layer interbedded with fine sand and silty clay; 2—$Q_p$: Gravel, sand, silt, clay; 3—$T_1$ Liucaiyuan Formation: purplish red, brick red, a small amount of gray green mudstone, glutenite, lithic sandstone; 4—$J_3$ Toutunhe Formation: purple iron argillaceous siltstone, gray-green fine-grained lithic sandstone mixed with mudstone; 5—$J_2$ Xishanyao Formation: gray green, light gray brown mudstone, argillaceous siltstone with coal line; 6—$J_1$ Sangonghe Formation: dark gray silty feldspar lithic sandstone; 7—$J_1$ Badaowan Formation: gray-green calcareous feldspathic lithic sandstone, a small amount of mudstone, siltstone coal line; 8—$P_3$ Hongyanchi Formation: gray black, dark gray argillaceous siltstone; 9—$T_1$ Shaofanggou Formation: purplish red glutenite, mudstone, lithic sandstone; 10—$T_2$ Member first of Karamay Formation: gray-green feldspar lithic sandstone and mudstone; 11—$T_3$ Huangshanjie Formation: yellow-green fine-grained lithic sandstone, greywacke, punctate mudstone; 12—$J_3$ Kalazha Formation: reddish brown pebbly lithic sandstone; 13—$P_3$ Lucaogou Formation: light gray, dark gray chlorite calcareous siltstone; 14—Zhizhu Hill; 15—Yamalik mountain; 16—Red Hill; 17—Railway; 18—Heping channel; 19—Measured main active faults; 20—Speculate active faults; 21—Indoor Radon survey location; 22—Soil Radon sampling site; 23—Long-term radon monitoring location .

 doi:10.20944/preprints202307.1754.v1



2.4.3. Radon Sampling Site Selection

Based on the comprehensive study of the geological, tectonic, and surface sediment characteristics in Urumqi, we did not employ a grid sampling approach. Instead, we focused on selecting radon survey sites in the areas where geological faults are active, including the Yamalike-Shuimogou Fault, the concealed fault in Wanyao Gou, the southern Hongshan Fault, as well as the vicinity of Yamalike Mountain and Zhizhu Hill located in geochemical uranium anomalies belt. Indoor radon and soil radon surveys should be carried out in areas where the soil is not disturbed as far as possible. The measured locations are shown in Figure 1.

## 3. Results

### *3.1. Indoor Radon and Thoron Characteristics*

From 2020 to 2023, a total of 151 instantaneous radon measurements using RAD7 and 32 cumulative radon measurements using SSNTD were conducted. The sampling sites were primarily located in residential buildings and offices in densely populated areas of Xinshi District, Economic Development Zone, Tianshan District, Shuimogou District, and Shayibake District. When conducting measurements in residential or office buildings, radon concentrations in the basements were measured simultaneously whenever possible.

3.1.1. Instantaneous Radon Concentrations

The statistics from a total of 151 measurements (excluding anomalous points) are listed in Table 1 and shown in Figure 2. Table 1 demonstrates a significant variation in $^{222}$Rn concentrations in both indoor and basement sites, with the arithmetic mean (AM) of $^{222}$Rn concentrations in the basement being 2.1 times higher than that of indoor $^{222}$Rn concentrations.

**Table 1.** Indoor radon concentration measurement by RAD7 (Bq/m3).

| Location | N | Ave | SD | Min | Max | Med | Geo* |
|---|---|---|---|---|---|---|---|
| Indoor | 106 | 90.24 | 83.04 | 11.73 | 485.58 | 69.24 | 66.25 |
| Basement | 34 | 189.50 | 175.1 | 18.67 | 632.60 | 157.61 | 115.27 |

* Denotes geometric mean values, the same below.

Excluding anomalous points and duplicate measurements, the arithmetic mean (AM) of indoor $^{222}$Rn concentrations from 106 sites is 90.24 ± 83.04 Bq/m$^3$, ranging from 11.7 to 486 Bq/m$^3$, with the median and geometric mean (GM) being 69.24 and 66.25 Bq/m$^3$, respectively. The AM in the basement is 2.1 times that in the dwellings. Both $^{222}$Rn concentrations indoor and in the basements present a lognormal distribution pattern, shown in Figure 2b,c. The highest $^{222}$Rn concentration of 486 Bq/m$^3$ was measured in the area of Yamalik Mountain. The $^{222}$Rn concentration in the three houses above 1000 Bq/m$^3$ were observed there, not included in Table 1.

Preprints (www.preprints.org) | NOT PEER-REVIEWED | Posted: 26 July 2023 doi:10.20944/preprints202307.1754.v1



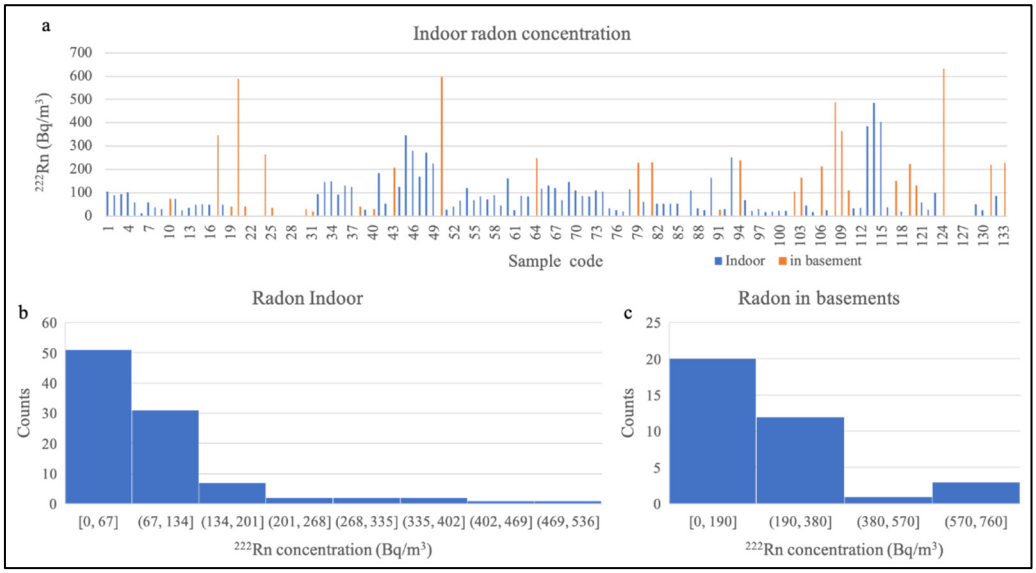


**Figure 2.** Measured Indoor radon concentration (**a**) and its statistical histogram (**b**,**c**).

In April 2021, $^{222}$Rn concentrations above 1000 Bq/m$^3$ were also observed in two basements of two buildings located near the intersection of the east-west and north-south fractures in Zhizhu Hill. This is an unconformity contact area of Qizigou Formation under Karaza Formation in the Lower Jurassic, where uranium is locally enriched in Qingshuihe Formation.

### 3.1.2. Long-term Cumulative Radon Measurements

To assess the reliability of the instantaneous radon measurement results in Urumqi, long-term cumulative radon measurements (using SSNTD) were conducted for a three- month period in the winters in 2022 and 2023. Out of the 32 measurement points, 50% of them were subjected to instantaneous measurements using RAD7. The comparison results are shown in Figure 3. Except for Site 4, the results by SSNTD are consistent with the values by RAD7 in Figure 3a, but the median and GM of SSNTD are higher than those of RAD7, shown in Figure 3b.

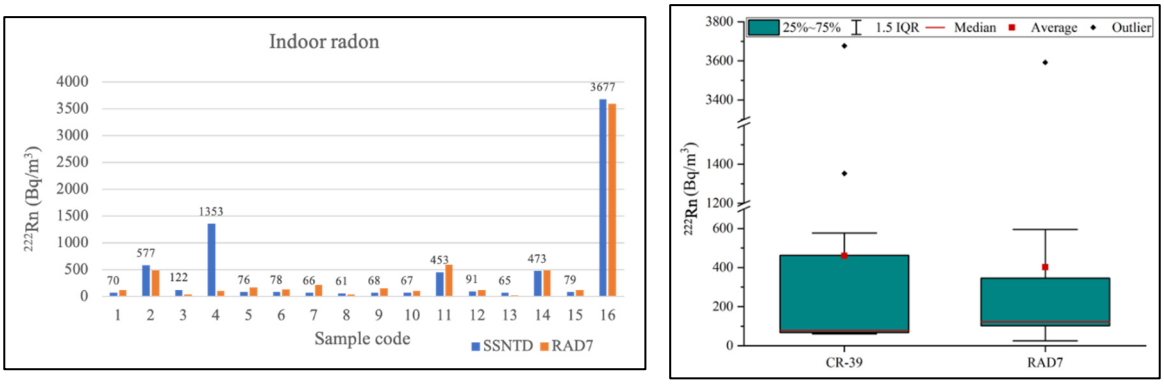


(**a**) (**b**)

**Figure 3.** Compassion of radon concentration by SSNTD and RAD7: (**a**) Bar charts; (**b**) Box diagram.

Table 2 presents the statistical data for indoor $^{222}$Rn and $^{220}$Rn concentrations determined using SSNTD. The arithmetic means (excluding anomalous points) for $^{222}$Rn and $^{220}$Rn concentrations are 166 ± 179 Bq/m$^3$ and 169 ± 155 Bq/m$^3$, respectively, with geometric means of 110 Bq/m$^3$ and 109 Bq/m$^3$, respectively. Indoor $^{222}$Rn concentrations greater than 1000 Bq/m$^3$ were observed in two hoses and one basement.

Preprints (www.preprints.org) | NOT PEER-REVIEWED | Posted: 26 July 2023 doi:10.20944/preprints202307.1754.v1



**Table 2.** Indoor radon and thoron concentration measurement by SSNTD (Bq/m³).

| Location | Isotope | N | Ave | SD | Min | Max | Med | Geo |
|---|---|---|---|---|---|---|---|---|
| Basement | $^{222}$Rn | 9 | 307 | 337 | 33 | 1080 | 185 | 174 |
| others | $^{222}$Rn | 22 | 205 | 311 | 31 | 1353 | 83 | 113 |
| Total | $^{222}$Rn | 29 | 166 | 179 | 31 | 685 | 79 | 110 |
| Total | $^{220}$Rn | 20 | 169 | 155 | 10 | 527 | 124 | 109 |

The $^{222}$Rn and $^{220}$Rn concentrations of whole measurements by SSNTD are shown in Figure 4. The indoor thoron concentration at Site 31 reaches as high as 1600 Bq/m³, but the reason for this anomaly is not yet clear. There is a possibility that it may be attributed to building materials, as no similar indoor thoron anomalies were observed in other dwellings within the same residential area.

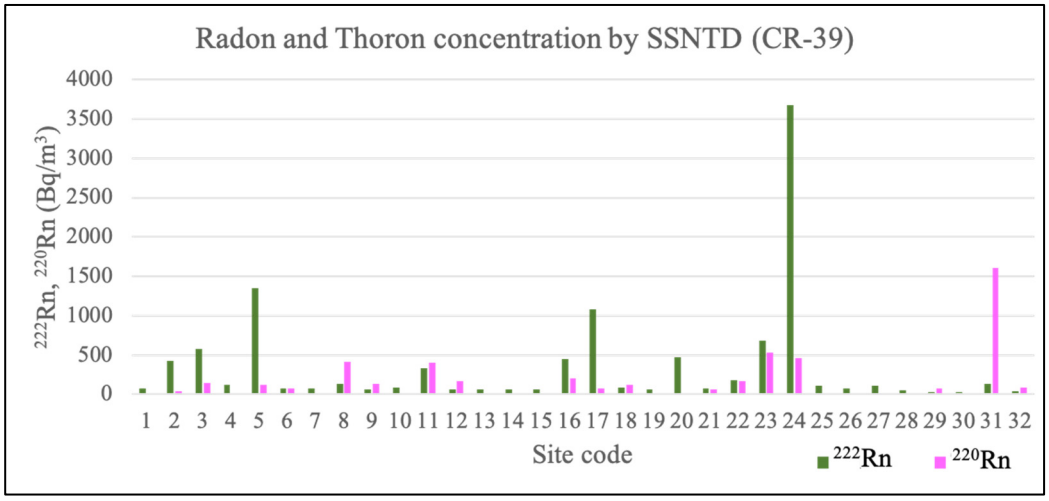


**Figure 4.** Radon and thoron concentration measured by SSNTD.

*3.2. Specific Activities of Uranium, Radium, and Cesium in Soil*

Table 3 presents the statistical results of the specific activities of uranium ($^{238}$U), radium ($^{226}$Ra), thorium ($^{232}$Th), and potassium-40 ($^{40}$K) and Cesium ($^{137}$Cs) in 45 soil samples from Urumqi.

**Table 3.** Uranium, radium, thorium, potassium-40, and Cesium radioactivity concentration (Bq/kg).

| | $^{238}$U | $^{226}$Ra | $^{232}$Th | $^{40}$K | $^{137}$Cs | k/(U/Ra) * |
|---|---|---|---|---|---|---|
| N | 45 | 45 | 45 | 45 | 30 | 44 |
| Ave | 41 | 45 | 41 | 855 | 4.42 | 1.01 |
| SD | 9 | 14 | 5 | 49 | 5.83 | 0.15 |
| Min | 22 | 27 | 26 | 757 | 0.14 | 0.81 |
| Max | 72 | 104 | 48 | 967 | 26.74 | 1.45 |

* k is the radioactive equilibrium coefficient of uranium and radium.

From Table 3, the following observations can be made:

1. The distribution of $^{238}$U, $^{226}$Ra, $^{232}$Th, and $^{40}$K in the soil samples is generally uniform. The distribution trends of $^{238}$U and $^{226}$Ra are consistent, shown as Figure 5. However, there are two higher values of $^{238}$U and $^{226}$Ra around Yamlik Mountain, where uranium mineralization was found during geological exploration of uranium deposits.
2. $^{137}$Cs radionuclides were detected in 30 out of 45 soil samples, but their specific activity varied widely. The average specific activity of $^{137}$Cs is 4.42 ± 5.83 Bq/kg, with the maximum of 26.74 Bq/kg. This suggests that 80% of the soil sampling points are located in relatively undisturbed natural soil layers.

Preprints (www.preprints.org) | NOT PEER-REVIEWED | Posted: 26 July 2023 doi:10.20944/preprints202307.1754.v1



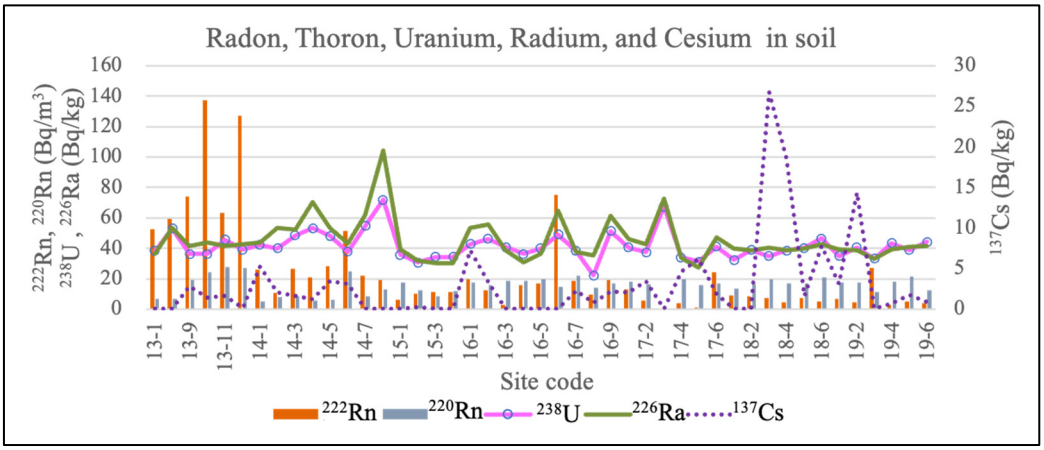


**Figure 5.** Specific activities of radon, thoron, uranium, radium, and cesium in soil.

*3.3. Distribution and Characteristics of Radon and Thoron in soil gas*

Soil radon measurements in Urumqi City were conducted in seven key research areas, including Yamalike Mountain, Zhizhu Hill, and other areas with well-developed geological structures and coal-bearing strata. The measured results of $^{222}$Rn and $^{220}$Rn of 45 out of 67 sites are shown in Figure 5, where soil samples were collected simultaneously.

The distribution of $^{222}$Rn and $^{220}$Rn in soil gas in Urumqi is uneven, and there are significant differences in different geological backgrounds. With the exception of R13 and R16, $^{222}$Rn concentrations at other regions were lower than 20 kBq/m$^3$. The AM of 65 measurements is 21.9 ± 20.5 kBq/m$^3$ after removing the $^{222}$Rn concentrations above 100 kBq/m$^3$. The maximum values observed of soil $^{222}$Rn and $^{220}$Rn are 137 kBq/m$^3$ and 27.8 kBq/m$^3$, respectively. This anomaly is located near zhizhu Hill, which is the unconformity contact between the Lower Jurassic Karaza Formation and the overlying Upper Cretaceous Qingshuihe Formation, where uranium mineralization was found.

## 4. Discussion

*4.1. The Specific Activities of Uranium and Radium in Soil Not Contributing to High Radon Potential*

Research data from both domestic and international studies indicate that areas with enriched uranium in surface soil are generally associated with high indoor radon potential, such as uranium deposit regions in Utah and Colorado in the United States, Czech Republic, and China [42–44]. Areas characterized by extensive outcrops of acidic granite and enrichment of heavy sand minerals, such as in Portugal, Yangjiang, and Zhuhai in China, also exhibit elevated uranium content [11,45,46]. Regions with higher uranium content also tend to have relatively higher radium specific activities. Radon, which is a decay product of radium, continuously emanates from rocks and soils and enters into soil pores. Radon migrates towards the surface under the influence of underground temperature and pressure and can enter indoor spaces through floor cracks and fissures. In areas with soil uranium content similar to Urumqi, such as Beijing and Shijiazhuang, the average indoor radon concentration is approximately 30 Bq/m$^3$ [47]. In Zhuhai, the average specific activity of uranium in soil is 63.6 ± 16.0 Bq/kg, with an average indoor radon concentration of 60 Bq/m$^3$, ranging from 1.23 to 154.2 Bq/m$^3$ [48,49]. In this survey, the average specific activities of uranium and radium in the 45 soil samples were 41 Bq/kg and 45 Bq/kg, respectively. Therefore, it can be concluded that the specific activities of uranium and radium in soil in Urumqi are not the primary factors contributing to elevated indoor radon levels in the area.

*4.2. Activity of Faults and Fault Structures as the Main Control Factor for Indoor Radon*

Compared with other inland cities, Urumqi shows significant differences in terms of topography, landform and climate. Within a range of 100 kilometers, there is a difference of 4954.4 m

between the highest and lowest altitude in Urumqi [36]. The region of Urumqi and its vicinity is known for numerous active faults, complex fault interactions, and intense tectonic activity, making it a frequent occurrence area for moderate to strong earthquakes [38]. The Tianshan Mountains are one of the youngest intracontinental mountain belts in the world and exhibit frequent and intense earthquake activity in Central Asia. From January 1 to October 31, 2020, Xinjiang experienced a total of 189 earthquakes of M3.0 and above, including two earthquakes of magnitude 6.0 to 6.9 [50,51]. The focal mechanism solutions provided by the United States Geological Survey (USGS) and the China Earthquake Networks Center (CENC) for the M6.0 earthquake in Kashi, Xinjiang, indicate that the earthquake was caused by thrust fault activity [52]. Strong earthquakes not only induce variations in local underground radon concentrations but also cause fluctuations in radon concentrations in groundwater over long distances. The 2008 Wenchuan earthquake, for example, resulted in anomalous radon concentrations in the groundwater of the Panzhihua Earthquake Observation Station [53,54]. The Tangshan Earthquake in 1976 and the earthquakes around Beijing from 1992 to 1996 also caused an increase in soil radon concentrations in Beijing [55,56]. In the investigation of concealed faults in Urumqi City, abnormal radon concentrations were observed in the soil above the fault in 9 out of 11 profiles [57]. The Yamalike-Shuimogou Fault, approximately 50 km in length, has a northeast trend and a southward dip with an inclination angle of 60-80 degrees. It is an active thrust fault zone [39]. In this study, the anomalous indoor radon and soil radon identified are located on the north and south flanks of the Yamalike anticline, influenced by the Yamalike Fault. Significant variations in indoor radon concentrations were also observed in basements near the Zhizhu Hill area. Radon from the deep subsurface enters the soil layer along the fault and fractured rocks under the influence of earthquake waves and then migrates into indoor spaces through cracks in basement walls and floors. Our data show that in the same building, the radon concentration in the undecorated basement is significantly higher than that in the decorated basement. Therefore, the activity of faults and fault structures are the main controlling factors for the elevated indoor radon levels in Urumqi, and the frequent occurrence of earthquake has led to an increase in average indoor radon concentrations.

### *4.3. Radon Escapes in Soil Gas*

The concentration of radon in soil is directly proportional to the radium activity in soil and is influenced by soil particle size, grain size, porosity, and soil moisture content [58–61]. During the weathering process, rock or mineral particles gradually decrease in size, leading to an increase in the specific surface area of the medium, which enhances radon emanation [62]. In areas with weathered granite, the soil radon concentration is significantly higher than in areas covered by Quaternary sediments [17].

Due to the large temperature difference between winter and summer in Urumqi, extensive weathering and erosion of the bedrock occur due to snow and ice meltwater. The soil has a low proportion of fine clay components, with an average content of coarse silt particles (particle size 0.01-0.05 mm) being the highest, followed by medium silt particles and fine silt particles. The content of coarse sand particles and fine clay particles is relatively low (less than 0.001 mm) [63]. Additionally, the presence of gravel in the soil and good connectivity between pores make it difficult to store free radon in the soil pores, leading to its easy emanation into the atmosphere. Furthermore, in mountainous or sloping areas, soil dryness and increased soil porosity make it challenging to achieve proper sealing of gas sampling holes during soil radon measurements. Improper field operations may result in underestimated soil radon measurements. This is the main reason for the low radon concentration in soil gas in Urumqi.

## 5. Conclusions and suggestions

In conclusion, based on our indoor instantaneous and long-term radon measurements, soil radon measurements, and radioactive activity analysis of uranium, radium, thorium, and potassium-40 in soil samples in representative areas of Urumqi, we have drawn the following conclusions:

1. The indoor radon concentration AM and GM in Urumqi are 90.24 ± 83.04 Bq/m$^3$ and 66.25 Bq/m$^3$, respectively, and the AM in basements is 2.1 times higher than that in dwellings. The mean radon value indoor in Urumqi is relatively high compared to the national average.
2. The results measured by SSNTD are consistent with the results of instantaneous radon measurements, but the AM by SSNTD is higher than that of instantaneous measurements, which may be related to the sampling conducted during winter.
3. The specific activities of uranium and radium in soil, as well as soil radon concentrations, are not the key factors contributing to elevated indoor radon levels. The activity of faults and tectonic structures is the main controlling factor affecting indoor radon concentration in Urumqi. Frequent earthquake has led to an increase in the average indoor radon concentration.
4. Some abnormal indoor radon values were observed in some buildings in Urumqi, but the source has not been identified. It is recommended to conduct more detailed investigations of indoor radon and the radioactivity of building materials in these regions.

**Supplementary Materials:** The following supporting information can be downloaded at the website of this paper posted on Preprints.org.

**Author Contributions:** Conceptualization, N.W.; methodology, N.W.; J.Y. software, H.W.; validation, N.W., H.W. and B.J.; formal analysis, H.W.; N.W.; J.Y.; investigation, H.W.; B.J; resources, J.Y.; data curation, H.W.; B.J; writing—original draft preparation, N.W.; J.Y; writing—review and editing, N.W.; A.P.; visualization, H.W.; project administration, N.W.; funding acquisition, N.W. All authors have read and agreed to the published version of the manuscript.

**Funding:** This research was funded by the National Natural Science Foundation of China, grant number 41974167.

**Institutional Review Board Statement:** The study did not require ethical approval.

**Informed Consent Statement:** Not applicable.

**Data Availability Statement:** The data presented in this study were uploaded as a Supplementary File.

**Acknowledgments:** The authors would like to thank Dr. Yunyun Wu, Institute of Radiation Protection and Nuclear Safety Medicine, Chinese Center for Disease Control and Prevention, for her assistance in conducting indoor radon measurement using solid state nuclear tracks detector. Thanks to Ying Jiang, a postgraduate student of China University of Geosciences (Beijing), for determining the specific activity of uranium and radium in soil samples.

**Conflicts of Interest:** The authors declare no conflict of interest.

## References

1. UNSCEAR. Sources and effects of ionizing radiation, united nations scientific committee on the effects of atomic radiation; UNSCEAR 2000 report to the general assembly, with scientific annexes, Volume I: Sources; United Nations: New York, NY, USA, 2000.
2. UNSCEAR. Sources to effects assessment for radon in homes and workplaces; UNSCEAR 2006 report to the general assembly, with scientific annexes, Volume II: Scientific Annexes E; United Nations: New York, NY, USA, 2006.
3. ICRP. Protection against radon-222 at home and at work; ICRP Publication 65, Ann. ICRP 23(2); Oxford: Pergamon Press, United Kingdom, 1993.
4. Ferlay, J.; Colombet, M.; Soerjomataram, I.; Dyba, T.; Randi, G.; Bettio, M.; Gavin, A.; Visser, O.; Bray, F. Cancer incidence and mortality patterns in Europe: Estimates for 40 countries and 25 major cancers in 2018. Eur. J. Cancer 2018, 103, 356-387. https://doi.org/10.1016/j.ejca.2018.07.005.
5. Gao, T.; Li, C.; Liang, X., Zheng, R.; Qiu, T. International Comparison of Cancer Incidence and Mortality in China. China Cancer 2016, 25, 409-414. https://doi.org/10.11735/j.issn.1004-0242.2016.06.A001. (In Chinese)
6. Åkerblom G. The use of airborne radiometric and exploration survey data and techniques in radon risk mapping in Sweden. Application of Uranium Exploration Data and Techniques in Environmental Studies; TECDOC-827; IAEA: Vienna, Austria, 1995; pp. 159-180.

7. Keller, G.; Schneiders, H.; Schütz, M.; Siehl, A.; Stamm, R. Indoor radon correlated with soil and subsoil radon potential—a case study. Environ. Geol. Water Sci 1992, 19, 113–119. https://doi.org/10.1007/BF01797439.
8. EPA. EPA's map of radon zones New York; USGS Open-file Report 93-292-B; Radon Division Office of Radiation and Indoor Air U.S. Environmental Protection Agency: New York, USA, 1993.
9. EPA. EPA's map of radon zones Vermont; EPA-402-R-93-085; Radon Division Office of Radiation and Indoor Air U.S. Environmental Protection Agency: Vermont, USA, 1993.
10. Alexander, W.G. Mapping indoor radon potential using geology and soil permeability. 1997 International Radon Symposium, Cincinnati, USA, Nov. 1997.
11. Wei, L. High background radiation research in Yangjiang China, Atomic Energy Press: Beijing, China, 1996.
12. Chen, B.; Guo, Q.; Sun, Q.; Zou, J. Survey on indoor 222Rn, 220Rn progeny in air in high background radiation area of Yangjiang, China. Radiation Protection 2006, 26, 50-55. https://doi.org/10.3321/j.issn:1000-8187.2006.01.008. (In Chinese)
13. Shang, B.; He, Q.; Wang, Z.; Zhu, C. Studies of indoor action level of radon in China. Chin. J. Radiol. Med. Prot. 2003, 23, 462-465. https://doi.org/10.3760/cma.j.issn.0254-5098.2003.06.032. (In Chinese)
14. Wang, N.; Xiao, L.; Li, C. The distribution and level of radon gas in soil in a high radiation background city of China. Geophysical and Geochemical Exploration 2012, 36, 646-650. https://doi.org/10.11720/wtyht.2012.4.27. (In Chinese)
15. Tang, L.; Zhu, L.; Hu, S.; Liu, Q. Study method on radon geological potential rules. Rock and Mineral Analysis 1999, 18, 1-6. https://doi.org/10.15898/j.cnki.11-2131/td.1999.01.001. (In Chinese)
16. Lu, W.; Wang, Z.; Gao, F.; Wang, R. Radon levels in the regional environment of Gejiu, Yunnan, and their relationship to the Geological Features. Environmental Science 1995, 16, 19-23. https://doi.org/10.13227/j.h.jkx.1995.02.007.
17. Wang, N.; Xiao, L.; Li, C.; Huang, Y.; Pei, S.; Liu, S.; Xie, F.; Cheng, Y. Determination of radioactivity level of 238U, 232Th and 40K in surface medium in Zhuhai City by in-situ Gamma-ray Spectrometry. Journal of Nuclear Science and Technology 2005, 42, 888-896. https://doi.org/10.1080/18811248.2005.9711040.
18. Lei, S.; Tokonami, S.; Sun, Q.; Ishikawa, T.; Kobayashi, Y.; Li, X.; Min, X.; Wu, G.; Yoshinaga, S.; Shang, B. Pilot study on indoor radon and thoron concentrations and terrestrial gamma doses in Gejiu, Yunnan province. China Occupational Medicine 2008, 35, 211-213. https://doi.org/10.3969/j.issn.1000-6486.2008.03.011. (In Chinese)
19. Shang, B.; Cui, H.; Yang, W. Radon and thoron concentrations in traditional cave dwellings and soil beds. Radiation Protection 2003, 23, 184-188, 192. https://doi.org/10.3321/j.issn:1000-8187.2003.03.008. (In Chinese)
20. Shang, B.; Wang, Z.; Gao, P.; Lei, S. Survey of radon concentrations in cave dwellings in the east of Gansu Province. Radiation Protection 1995, 15, 461-463.
21. Ren, T. Source, level and control of indoor radon. Radiation Protection 2001, 21, 291-299. (In Chinese)
22. The writing group of the summary report on nationwide survey of environmental radioactivity level in China. Survey of concentrations of radon and $\alpha$ potential energy of Rn daughter products in air in some regions of China (1983-1990). Radiation Protection 1992, 12, 164-171. (In Chinese)
23. Xu, D.; Shang, B.; Cao, Z. Investigation of key indoor air pollutants in residence in part of the cities in China. Journal of Hygiene Research 2007, 36, 473-476. https://doi.org/10.3969/j.issn.1000-8020.2007.04.019. (In Chinese)
24. Shang, B.; He, Q.; Wang, Z.; Zhu, C. Studies of indoor action level of radon in China. Chinese Journal of Radiological Medicine and Protection 2003, 23, 462-465. https://doi.org/10.3760/cma.j.issn.0254-5098.2003.06.032. (In Chinese)
25. Shang, B.; Cui, H.; Zhang, L.; Chen, B.; Wu, J.; Wang, Y.; Gao, Y.; Chen, H.; Li, Z.; Wang, M.; Z.; et al. Investigation of indoor radon concentration in a typical area of China by solid tracer method. Chinese Society of Nuclear Physics. Proceedings of the Eighth National Conference on Solid State Nuclear Tracing, Xiamen, China, Jun. 2004.
26. Wang, C.; Pan, Z.; Liu, S.; Yang, M.; Shang, B.; Zhuo, W.; Ren, T.; Xiao, D.; Yang, W.; Li, F.; et al. Investigation on indoor radon levels in some parts of China. Radiation Protection 2014, 34, 65-73. (In Chinese)

27. Zhu, W.; Lin, J.; Li, Z.; Lei, S.; Sun, X.; Liu, F. Investigation on radon concentration in Urumqi metro line 1. Bull. Dis. Control Prev. (China) 2021, 36, 59-60+72. https://doi.org/10.13215/j.cnki.jbyfkztb.2105001. (In Chinese)
28. Wang, X.; Jin, Y.; Chen, Z.; et al. China indoor radon study; Science Press: Beijing, China, 2013. (In Chinese)
29. Han, Q.; Lv, A.; Su, J. Reinvestigation on influence parameters of indoor radon concentration in Urumqi and relevant countermeasures. Radiation Protection 2012, 32, 171-176+192. (In Chinese)
30. Tu, Q.; Xie, N.; Wei, Z.; et al. The Report of the 1/250,000 multi-target regional geochemical survey in Urumqi-Changji area. National Geological Library, 2011. https://doi.org/10.35080/n01.c.119322. (In Chinese)
31. Su, J.; Xu, M.; Li, M.; Guo, Y.; Han, Q. Investigation on soil radon concentration levels and distribution in Urumqi. Radiation Protection 2009, 29, 327-333. (In Chinese)
32. Wang, N.; Peng, A.; Xiao, L.; Chu, X.; Yin, Y.; Qing, C.; Zheng, L. The level and distribution of 220Rn concentration in soil-gas in Guangdong Province, China. Radiat. Prot. Dosim. 2012, 152, 204-209. https://doi.org/10.1093/rpd/ncs223.
33. Wang, N.; Zheng, L.; Chu, X.; Li, S.; Yan, S. The characteristics of radon and thoron concentration from soil gas in Shenzhen City of Southern China. Nukleonika 2016, 61, 315-319. https://doi.org/10.1515/nuka-2016-0052.
34. Wu, Y.; Cui, H.; Zhang, Q.; Shang, B. Intercomparisons for integrating the radon–thoron detector of NIRP, China with NIRS, Japan. Radiation Protection Dosimetry 2015, 164, 398-401. https://doi.org/10.1093/rpd/ncu286.
35. State Administration for Market Regulation of the People's Republic of China, Standardization administration of the People's Republic of China. Gamma-ray spectrometry method for the determination of radionuclides in environmental and biological samples; GB/T 16145-2022; Standards Press of China: Beijing, China, 2022. (In Chinese)
36. Overview of Urumqi. Available online: http://www.urumqi.gov.cn/wlmjgk/447021.htm (access on 5 Jun. 2023).
37. Waheiti, W.; Ren, G.; Sun, X. The daily temperature characteristics of the intensity of urban heat island in Urumqi and seasonal changes. Desert and Oasis Meteorology, 2018, 12, 21-28.
38. Zhang, H.; Xie, F.; Cui, X.; Du, Y.; Shu, S. Active fault sliding and recent tectonic stress field in the Urumqi area. Earthquake Research in China 2006, 22, 259-268. https://doi.org/10.3969/j.issn.1001-4683.2006.03.006. (In Chinese)
39. Ye, M.; Su, N. Active faults and urban construction. City Disas. Reduc. 2004, 4, 13-16. https://doi.org/10.3969/j.issn.1671-0495.2004.04.005. (In Chinese)
40. Yang, F. The geologic structure and earthquake movement in the area of Urumqi. Journal of Xinjiang Normal University (Natural Sciences Edition) 1990, 2, 84-89. (In Chinese)
41. Tang, L.; Shen, J.; Liu, Z. Determination of potential seismic source in Urumqi region and its periphery. Inland Earthquake 2010, 24, 8-12. https://doi.org/10.3969/j.issn.1001-8956.2010.01.002. (In Chinese)
42. Cui, L. Radiometric methods in regional radon hazard mapping. Geophysical and Geochemical Exploration Abroad 1991, 4, 18-24. (In Chinese)
43. Cui, L. Some results of radon hazard investigations. Geological Review 1994, 40, 157-164. https://doi.org/10.3321/j.issn:0371-5736.1994.02.009. (In Chinese)
44. Gan, N.; Cen, K.; Ye, R.; Li, T. Rapid estimation of environmental radioactivity surrounding Xiangshan uranium deposits, Jiangxi province, Eastern China. Nukleonika 2018, 63, 113-121. https://doi.org/10.2478/nuka-2018-0014.
45. Carvalho, F.P.; Madruga, M.J.; Reis, M.C.; Alves, J.G.; Oliveira, J.M.; Gouveia, J.; Silva, L. Radioactivity in the environment around past radium and uranium mining sites of Portugal. J. Environ. Radioact. 2007, 96, 39–46. https://doi.org/10.1016/j.jenvrad.2007.01.016.
46. Yuan, Y.; Morishima, H.; Shen, H.; Mioko, K.; Wei, L.; Jian, Y. Estimation of doses to the residents arising from inhalation of Rn-222, Rn-220 and their decay products in high background radiation area of Yangjiang. Chin. J. Radiol. Health 2002, 11, 65-68. https://doi.org/10.13491/j.cnki.issn.1004-714x.2002.02.002. (In Chinese)
47. Qin, C.; Wang, N.; Xiao, L.; Chu, X. The correlation between indoor radon concentrations and geological backgrounds in some typical areas of Beijing and Guangdong. Geophysical and Geochemical Exploration 2012, 36, 441-444. https://doi.org/10.11720/wtyht.2012.3.23.

48. Guo, Q.; Cheng, J. Measurement of 222Rn/220Rn progeny and exhalation rates for 222Rn/220Rn from soil in Zhuhai area. Radiation Protection 2004, 24, 110-115. https://doi.org/10.3321/j.issn:1000-8187.2004.02.005. (In Chinese)
49. Xiao, L.; Wang, N.; Li, C.; Liu, S.; Huang, Y.; Liu, D. Indoor concentration of 222Rn in Zhuhai typical area. The Third National Symposium on Natural Radiation Exposure and Control, Baotou, Inner Mongolia, China, 29 Aug. 2010.
50. In the first 10 months of this year, 513 earthquakes of magnitude 3 or higher occurred in China. Available online: https://news.sina.com.cn/c/2020-11-01/doc-iiznezxr9270929.shtml (access on 9 Feb. 2023)
51. Guangdong Earthquake Agency. http://www.gddzj.gov.cn/gddzj/dzpd/yzqgk/714752/index.html (access on 6 Jun. 2023).
52. Yao, Y.; Li, T.; Liu, Q.; Di, N. Characteristics of geological hazards in the epicenter of the Jiashi Mw6.0 earthquake on January 19, 2020. Seismology and Geology 2021, 2, 410-429. https://doi.org/10.3969/j.issn.0253-4967.2021.02.010. (In Chinese)
53. Alam, A.; Wang, N.; Zhao, G.; Barkat, A. Implication of Radon Monitoring for Earthquake Surveillance Using Statistical Techniques: A Case Study of Wenchuan Earthquake. Geofluids 2020, 2020, 1-14. https://doi.org/10.1155/2020/2429165.
54. Alam, A.; Wang, N.; Petrak, E.; Barkat, A.; Huang, F.; Shah, M.A.; Cantzos, D.; Priniotakis, G.; Yannakopoulos, P.H.; Papoutsidakis, M.; et al. Fluctuation Dynamics of Radon in Groundwater Prior to the Gansu Earthquake, China (22 July 2013: Ms= 6.6): Investigation with DFA and MFDFA Methods. Pure Appl. Geophys. 2021, 178, 3375-3395. https://doi.org/10.1007/s00024-021-02818-8.
55. Du, J.; Yu, W.; Li, S.; Jian, C.; Zhu, Z.; Chen, H.; Kang, C. The geochemical characteristics of escaped radon from the Babaoshan fault zone and its earthquake reflecting effect. Earthquake 1998, 18, 155-162. (In Chinese)
56. Zhou, Z.; Zhao, F.; Li, Y.; Zhou, X.; Han, X. Radon environmental geochemistry in soil gas around the Capital area of China. Chinese Journal of Ecology 2014, 33, 1729-1733. https://doi.org/10.13292/j.1000-4890.20140429.006. (In Chinese)
57. Wang, D.; Zhang, Y.; Zhang, H. Gas geochemical survey of concealed faults in the city proper of Urumqi. Inland Earthquake 1999, 13, 143-152. https://doi.org/10.16256/j.issn.1001-8956.1999.02.009. (In Chinese)
58. Adler, P.M.; Perrier, F. Radon emanation in partially saturated porous media. Transport in Porous Media 2009, 78, 149-159. https://doi.org/10.1007/s11242-008-9291-z.
59. Breitner, D.; Arvela, H.; Hellmuth, K.-H.; Renvall, T. Effect of moisture content on emanation at different grain size fractions-A pilot study on granitic esker sand sample. Journal of environmental radioactivity 2010, 101,1002-1006. https://doi.org/10.1016/j.jenvrad.2010.07.008.
60. Megumi, K.; Mamuro, T. Emanation and exhalation of radon and thoron gases from soil particles. J. Geophys. Res. 1974, 79, 3357-3360. https://doi.org/10.1029/JB079i023p03357.
61. Megumi, K.; Mamuro, T. Concentration of uranium series nuclides in soil particles in relation to their size. J. Geophys. Res. 1977, 82, 353-356. https://doi.org/10.1029/JB082i002p00353.
62. Sakoda, A.; Nishiyama, Y.; Hanamoto, K.; Ishimori, Y.; Yamamoto, Y.; Kataoka, T.; Kawabe, A.; Yamaoka, K. Differences of natural radioactivity and radon emanation fraction among constituent minerals of rock or soil. Appl. Radiat. Isot. 2010, 68, 1180-1184. https://doi.org/10.1016/j.apradiso.2009.12.036.
63. Quan, T.; Chen, X.; Li, Y.; Yang, H. Soil Physicochemical Characteristics at Different Land Use Types in Urumqi. Journal of Northwest Forestry University 2016, 5, 37-42. https://doi.org/10.3969/j.issn.1001-7461.2016.05.06. (In Chinese)